

Plasmonic reflection grating back contacts for microcrystalline silicon solar cells

U. W. Paetzold, E. Moulin, D. Michaelis, W. Böttler, C. Wächter et al.

Citation: *Appl. Phys. Lett.* **99**, 181105 (2011); doi: 10.1063/1.3657513

View online: <http://dx.doi.org/10.1063/1.3657513>

View Table of Contents: <http://apl.aip.org/resource/1/APPLAB/v99/i18>

Published by the [American Institute of Physics](http://www.aip.org).

Additional information on *Appl. Phys. Lett.*

Journal Homepage: <http://apl.aip.org/>

Journal Information: http://apl.aip.org/about/about_the_journal

Top downloads: http://apl.aip.org/features/most_downloaded

Information for Authors: <http://apl.aip.org/authors>

ADVERTISEMENT



AIP | Applied Physics Letters

Accepting Submissions in
Biophysics and Bio-Inspired Systems

Submit Today

AIP
Publishing

Plasmonic reflection grating back contacts for microcrystalline silicon solar cells

U. W. Paetzold,^{1,a)} E. Moulin,¹ D. Michaelis,² W. Böttler,¹ C. Wächter,² V. Hagemann,³ M. Meier,¹ R. Carius,¹ and U. Rau¹

¹EK5-Photovoltaik, Forschungszentrum Juelich GmbH, D-52425 Juelich, Germany

²Fraunhofer Institut für Angewandte Optik und Feinmechanik, Albert Einstein Str. 7, D-07745 Jena, Germany

³Schott AG, Hattenbergstr. 10, D-55122 Mainz, Germany

(Received 4 August 2011; accepted 12 October 2011; published online 31 October 2011)

We report on the fabrication and optical simulation of a plasmonic light-trapping concept for microcrystalline silicon solar cells, consisting of silver nanostructures arranged in square lattice at the ZnO:Al/Ag back contact of the solar cell. Those solar cells deposited on this plasmonic reflection grating back contact showed an enhanced spectral response in the wavelengths range from 500 nm to 1000 nm, when comparing to flat solar cells. For a particular period, even an enhancement of the short circuit current density in comparison to the conventional random texture light-trapping concept is obtained. Full three-dimensional electromagnetic simulations are used to explain the working principle of the plasmonic light-trapping concept. © 2011 American Institute of Physics. [doi:10.1063/1.3657513]

High-performance thin-film silicon solar cells require advanced light-trapping concepts to enhance the absorption of light in the optically thin silicon absorber layers.^{1,2} The conventional random texture light-trapping concept makes use of light scattering and diffraction at randomly textured interfaces of the transparent front contact and of reflective back contacts.¹⁻⁴ The random textures are realized on various materials including wet-chemically etched ZnO:Al layers and as-deposited grown SnO₂ and ZnO:Al layers.³⁻⁶ As for all of these textures the spectral response of thin-film silicon solar cells remains significantly below the theoretical limits, several new light-trapping concepts have been investigated recently. Two promising concepts are (i) surface gratings which allow for a control of the scattering angles via discrete diffraction orders⁷⁻¹¹ and (ii) Ag nanostructures of radii above 100 nm which scatter incident light at high efficiencies and low absorption via localized surface plasmon polaritons.¹²⁻¹⁷

In this letter, these two concepts are combined in the *plasmonic reflection grating back contact*. Half-ellipsoidal Ag nanostructures are arranged in square lattice at the ZnO:Al/Ag back contact of microcrystalline silicon (μ c-Si:H) solar cells, such that they form a two-dimensional reflection grating (Fig. 1). For the applied dimensions of the half-ellipsoidal Ag nanostructures, plasmonic resonances are known to induce enhanced scattering for wavelengths between 500 nm and 1000 nm.¹⁷ For ultrathin amorphous silicon solar cells deposited strictly conformal on a similar back contact structure, enhancements of the solar cell performance have been reported by Ferry *et al.*¹⁴ The present work investigates plasmonic reflection grating back contacts in μ c-Si:H solar cells, which are of particular interest as highest efficiencies for thin-film silicon solar cells are obtained today using multi-junction concepts with μ c-Si:H bottom cells.^{1,18} Furthermore, the μ c-Si:H solar cells investi-

gated here have an absorber layer thickness above 1000 nm such that the front and rear side of the cell can be regarded in first approximation as separate optical units which are not connected via electromagnetic near-field effects, i.e., both sides are evanescently decoupled.

In order to demonstrate the plasmonic light-trapping concept of plasmonic reflection grating back contacts, n-i-p substrate-type μ c-Si:H solar cells with an active cell area of 0.25 cm² were fabricated. First, nanostructured substrates with square lattice arranged nano-cubes were prepared with an imprint process. On top of these substrates, a 200 nm thick Ag layer and afterwards a 80 nm thick ZnO:Al layer was deposited by radio-frequency-sputtering. Due to the nearly conformal deposition of Ag, the surface reveals half-ellipsoidal nanostructures of radii around 110 nm and of height around 80 nm, forming the plasmonic reflection grating back contact surface [cf. Fig. 1(b)]. Afterwards, the μ c-Si:H layer stack was deposited by plasma enhanced chemical vapor deposition. The n-doped, intrinsic, and p-doped μ c-Si:H layers have thicknesses of 11 nm, 1082 nm, and 20 nm, respectively. As front contact we use an around 60 nm to 70 nm

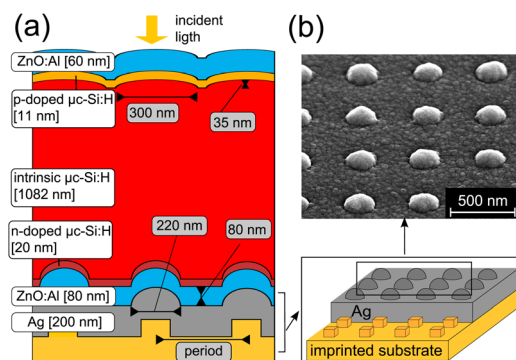


FIG. 1. (Color online) (a) Cross-section of the n-i-p substrate type μ c-Si:H solar cell with integrated plasmonic reflection grating back contact. (b) Scanning electron microscopy image of the plasmonic reflection grating surface.

^{a)} Author to whom correspondence should be addressed. Electronic mail: u.paetzold@fz-juelich.de.

thick ZnO:AL layer in combination with Ag finger electrodes. For comparison, additional solar cells were deposited under the same conditions on flat and randomly textured glass/ZnO:Al substrates. To ensure the comparability of the $\mu\text{c-Si:H}$ material, the crystallinity was determined by Raman measurements. The random texture was induced by wet-chemical etching of ZnO:Al for 45 s in 0.5 w/w % HCl, resulting in a surface roughness of root mean square of 139 nm (for more details see Ref. 4).

An appropriate measure for the light-trapping effect in the solar cells is the external quantum efficiency (*EQE*) in the semitransparent region of the intrinsic $\mu\text{c-Si:H}$ layer (wavelengths between 500 nm and 1000 nm). By convolving the *EQE* with the AM1.5 spectrum, the J_{sc} is calculated which is directly proportional to the efficiency of the solar cell. Figure 2(a) shows the measured *EQE* spectra of three $\mu\text{c-Si:H}$ solar cells deposited at the same conditions on (i) a flat back contact, (ii) a random texture back contact, and (iii) a plasmonic reflection grating back contact with square lattice period of 500 nm. For wavelengths from 550 nm to 1000 nm, the *EQE* of the solar cell deposited on the plasmonic reflection grating back contact is significantly enhanced in comparison to the *EQE* of the solar cell deposited on the flat back contact. The enhancement shows that the plasmonic reflection grating back contact is capable of scattering a substantial amount of incident light inside the $\mu\text{c-Si:H}$ absorber layer of the solar cell, leading to an enhanced generation of charge carriers. As a result, the plasmonic light-trapping concept enhances the J_{sc} from 17.7 mA/cm² to 21.0 mA/cm². For comparison, the highest J_{sc} measured at a solar cell deposited on the random texture back contact is only 20.8 mA/cm². In particular, in the wavelength range from 580 nm to 800 nm, the plasmonic light-trapping concept leads to a strongly enhanced averaged *EQE* in comparison to the random texture light-trapping concept [Fig. 2(a)].

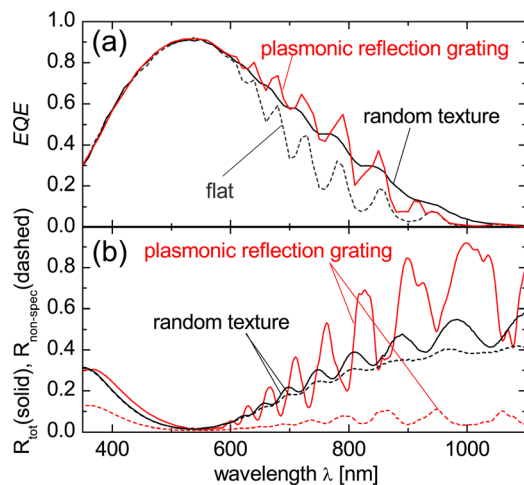


FIG. 2. (Color online) (a) Measured *EQE* of $\mu\text{c-Si:H}$ solar cells with integrated flat back contact, random texture back contact, and plasmonic reflection grating back contact. (b) Non-specular reflection ($R_{non-spec}$) and total reflection (R_{tot}) of solar cells with integrated random texture back contact and plasmonic reflection grating back contact. For the latter device, the non-specular contribution beyond 500 nm arises from remaining cell roughness and irregularities which also explain the only weakly observable resonance anomalies in the *EQE* and R_{tot} .

To compare the optical properties of both concepts, the measured total and non-specular reflection of the corresponding solar cells are shown in Fig. 2(b). For the solar cell deposited on the random texture back contact, most of the reflected light is diffusively reflected. For this solar cell, light-trapping is obtained by scattering incident light at the randomly textured interfaces into broad angle distributions in the $\mu\text{c-Si:H}$ absorber layer.² Consequently, also the light reflected from the solar cell is mostly reflected diffusively (i.e., non-specularly). In contrast, the light reflected at the solar cell deposited on the plasmonic reflection grating back contact is mostly reflected specularly. Thus, the working principle of the plasmonic light-trapping concept differs from the random texture light-trapping concept.

In order to explain the working principle of the plasmonic light-trapping concept, optical simulations of solar cells and back contact layer stacks were conducted with a 3D numerical solver. The applied software (JCMsuite) is based on the finite element method and discretizes Maxwell's equations on a prismatic grid.¹⁹ From the simulated 3D electromagnetic field distributions, absorption profiles and angular resolved scattering intensity distributions were calculated. The *EQE* of the simulated solar cells was calculated assuming that every photon absorbed in the intrinsic $\mu\text{c-Si:H}$ layer and 50% of the photons absorbed in the n-doped layer contribute to the J_{sc} . The optical data of the simulated layers were taken from measurements of state of the art solar cell materials. A cross-section of the simulated solar cell and the plasmonic reflection grating back contact is shown in Fig. 1. The geometric shapes and numbers were taken from scanning electron microscopy images of cross-sections of the experimentally realized solar cells (prepared by focused ion beam). Due to the non-conformal growth of the $\mu\text{c-Si:H}$, the surface structure of the substrate is levelled at the front side.

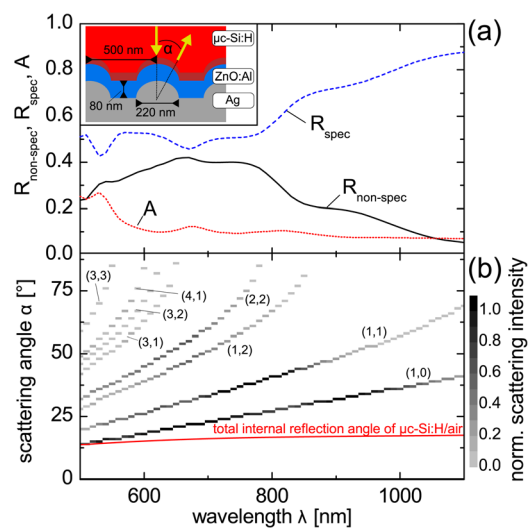


FIG. 3. (Color online) (a) Non-specular reflection ($R_{non-spec}$), specular reflection (R_{spec}) and absorption (A) calculated from 3D simulations of the plasmonic reflection grating back contact shown in the inset. (b) Scattering intensity distribution of the diffuse reflected light within the diffraction orders of the plasmonic reflection grating as a function of the scattering angle and the wavelength. Light scattered beyond the total internal reflection angle of $\mu\text{c-Si:H/air}$ (red line) will be reflected totally at a flat front side of the solar cell.

Figure 3(a) shows the simulated absorption and reflection as well as the simulated scattering intensity distribution of the non-specularly reflected light of the plasmonic reflection grating back contact. In the entire wavelength range from 500 nm to 1000 nm, a substantial amount of incident light at the back contact is reflected non-specularly. In particular, for wavelengths between 580 nm and 800 nm, where an enhanced *EQE* in comparison to the random texture light-trapping concept was observed (Fig. 2), more than 35% of incident light is scattered. The absorption at the back contact remains below 12%. Due to the periodic arrangement of the nanostructures, the non-specularly reflected light at the plasmonic reflection grating back contact is scattered into discrete diffraction orders [Fig. 3(b)]. Importantly, for wavelengths longer than 500 nm, the minimum scattering angles of these diffraction orders are larger than the total reflection angle of a flat $\mu\text{c-Si:H}$ /air interface. As a result, the light path of the light scattered into the diffraction orders in the intrinsic $\mu\text{c-Si:H}$ layer is enhanced twofold. First, the light path is simply enhanced by the scattering angle. Second, considering the nearly flat front interface of the solar cell incident light which is scattered at the plasmonic reflection grating back contact to angles beyond the angle of total reflection of the $\mu\text{c-Si:H}$ /air interface will be reflected totally at the front side. In other words, the light is coupled into the waveguide modes of the layer stack. The resulting enhanced light path leads to an enhanced *EQE* and J_{sc} . Furthermore, due to the reciprocity of all light paths, such light reflected totally at the front side will be either reflected or scattered antiparallel to normal incidence at its second incidence on the plasmonic reflection grating back contact, i.e., causing a decoupling from the waveguide modes. Therefore, the reflected and reemitted light from the solar cell deposited on a plasmonic reflection back contact must be mostly specular [cf. Fig. 2(b)]. The resonance anomalies generally occurring for waveguide mode excitation are not apparent in the measurements due to remaining roughness and material irregularities.

Figure 4 shows the simulated and experimental J_{sc} of $\mu\text{c-Si:H}$ solar cells deposited on plasmonic reflection grating back contacts of square lattice periods between 500 nm and 1000 nm. For all periods, qualitatively similar *EQE* enhancements are found in the wavelength range from 550 nm to 1000 nm (not shown). The largest enhancement of J_{sc} for the given solar cell structures is found for a period of 500 nm. Only for this period an enhancement of J_{sc} in comparison to the solar cells deposited on the random texture back contact is observed. With increasing period the measured J_{sc} decreases. This decrease was also observed for the J_{sc} calculated from 3D simulations. We explain this decrease of J_{sc} by two effects. First, the surface coverage of the scattering Ag nanostructures decreases with increasing period. Second, the scattering angles of the diffraction orders of the plasmonic reflection grating decrease with increasing period, resulting in less efficient light-trapping effect. The simulated absolute values of J_{sc} agree well with the measured data, allowing for a future optimization of geometrical parameters (e.g., size, shape of the nanostructures).

To conclude, a plasmonic light-trapping concept based on plasmonic reflection grating back contacts was implemented

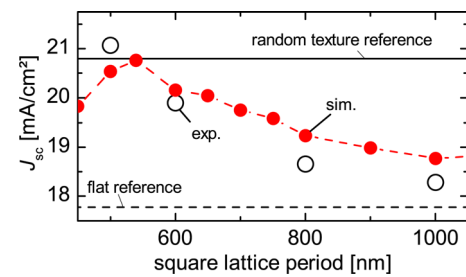


FIG. 4. (Color online) Measured and simulated short circuit current densities (J_{sc}) of $\mu\text{c-Si:H}$ solar cells with integrated plasmonic reflection grating back contacts of various square lattice periods.

in $\mu\text{c-Si:H}$ thin-film solar cells. In this concept, efficiently scattering and weakly absorbing Ag nanostructures arranged in square lattice at the back contact scatter incident light to large angles in the $\mu\text{c-Si:H}$ absorber layer, resulting in a significantly enhanced *EQE*. For an optimized period of the plasmonic reflection grating, an enhancement of J_{sc} in comparison to the conventional random texture light-trapping concept was found. Applying optical simulations the working principle of the plasmonic light-trapping concept was explained.

The authors thank M. Prömpers, K. Bittkau, B. E. Pieters, F. Fingers, G. von Plessen, and S. Burger for helpful discussions. This work was supported by the German Federal Ministry of Education and Research (contract 03SF0354D).

- ¹B. Rech, T. Repmann, M. N. van den Donker, M. Berginski, T. Kilper, J. Hüpkens, S. Calnan, H. Stiebig, and S. Wieder, *Thin Solid Films* **511–512**, 548 (2006).
- ²R. H. Franken, R. L. Stolk, H. Li, C. H. M. van der Werf, J. K. Rath, and R. E. I. Schropp, *J. Appl. Phys.* **102**, 014503 (2007).
- ³J. Meier, U. Kroll, J. Spitznagel, S. Benagli, T. Roschek, G. Pfanner, C. Ellert, G. Androusoyopoulos, A. Hugli, M. Nagel, C. Bucher, L. Feitknecht, G. Buchel, and A. Buchel, in *Proc. IEEE 2005 PV Spec. Conf.* IEEE, Piscataway, New Jersey, USA (2005), pp. 1464–1467.
- ⁴J. Müller, B. Rech, J. Springer, and M. Vanecek, *Sol. Energy* **77**, 917 (2004).
- ⁵T. Matsui, M. Tsukiji, H. Saika, T. Toyama, and H. Okamoto, *J. Non-Cryst. Solids* **299–302**, 1152 (2002).
- ⁶T. Söderström, F.-J. Haug, X. Niquille, and C. Ballif, *Prog. Photovoltaics* **17**, 165 (2009).
- ⁷C. Heine and R. Morf, *Appl. Opt.* **34**, 2476 (1995).
- ⁸H. Stiebig, N. Senoussaoui, C. Zahren, C. Haase, and J. Müller, *Prog. Photovoltaics* **14**, 13 (2006).
- ⁹H. Sai and M. Kondo, *J. Appl. Phys.* **105**, 094511 (2009).
- ¹⁰K. Söderström, F. J. Haug, J. Escarré, O. Cubero, and C. Ballif, *Appl. Phys. Lett.* **96**, 213508 (2010).
- ¹¹K. R. Catchpole and A. Polman, *Appl. Phys. Lett.* **93**, 191113 (2008).
- ¹²Hallermann, C. Rockstuhl, S. Fahr, G. Seifert, S. Wackerow, H. Graener, G. v. Plessen, and F. Lederer, *Phys. Status Solidi A* **202**, 2844 (2008).
- ¹³H. A. Atwater and A. Polman, *Nature Mater.* **9**, 205 (2010).
- ¹⁴V. E. Ferry, M. A. Verschuuren, H. B. T. Li, E. Verhagen, R. J. Walters, R. E. I. Schropp, H. A. Atwater, and A. Polman, *Opt. Express* **18**, 102 (2010).
- ¹⁵E. Moulin, J. Sukmanowski, P. Lou, R. Carius, F. X. Royer, and H. Stiebig, *J. Non-Cryst. Solids* **354**, 2488 (2008).
- ¹⁶U. Kreibig and M. Vollmer, *Optical Properties of Metal Clusters* (Springer, Berlin, 1995).
- ¹⁷U. W. Paetzold, E. Moulin, K. Bittkau, B. E. Pieters, R. Carius, and U. Rau, in *Proceedings of the 25th EUPVSEC*, WIP, Munich, Germany (2011), p. 3036.
- ¹⁸M. A. Green, K. Emery, Y. Hishikawa, and W. Warta, *Prog. Photovoltaics* **19**, 84 (2011).
- ¹⁹J. Pomplun, S. Burger, L. Zschiedrich, and F. Schmidt, *Phys. Status Solidi B* **244**, 3419 (2007).